

Article

# Influence of Acetonitrile on the Electrochemical Behavior of Ionic Liquid-Based Supercapacitors

Boryana Karamanova, Luybomir Sosarov, Elefteria Lefterova, Toma Stankulov  and Antonia Stoyanova \*

Institute of Electrochemistry and Energy Systems, Bulgarian Academy of Sciences, G. Bonchev Str. 10, 1113 Sofia, Bulgaria; borianka.karamanova@ees.bas.bg (B.K.); l\_stefanov@ees.bas.bg (L.S.); edl@ees.bas.bg (E.L.); tstankulov@ees.bas.bg (T.S.)

\* Correspondence: antonia.stoyanova@ees.bas.bg

**Abstract:** The creation of supercapacitors with superior energy density and power capabilities is critical for advanced energy storage solutions. Ionic liquid electrolytes offer a promising alternative in this respect. However, improving their cycle stability and efficiency is a complex task requiring extensive research and significant effort. The high viscosity of ionic liquids (ILs) limits their lifetime, but this can be mitigated by increasing the temperature or adding solvents. In this research, the electrochemical performance of symmetric activated carbon supercapacitors with 1-Ethyl-3-methylimidazolium tetrafluoroborate (EMIMBF<sub>4</sub>) and different ratios of acetonitrile (ACN) as electrolytes were investigated. Long-term galvanostatic charge/discharge tests, impedance studies, and cyclic voltammetry were performed at temperatures between 24 to 60 °C. The addition of ACN to the ionic liquid increased electrochemical stability and reduced internal resistance, with the best performance observed at a 1:2 volume ratio of EMIMBF<sub>4</sub> to ACN. This supercapacitor exhibited 87% cyclic stability after 5000 charge/discharge cycles in the voltage range of 0.05–2.8 V and a current rate of 1 A g<sup>-1</sup>. It also achieved an energy density of 23 Wh kg<sup>-1</sup> and a power density of 748 W kg<sup>-1</sup>. The supercapacitors were stable at elevated temperatures up to 60 °C, showing no degradation after operation under various thermal conditions.



**Citation:** Karamanova, B.; Sosarov, L.; Lefterova, E.; Stankulov, T.; Stoyanova, A. Influence of Acetonitrile on the Electrochemical Behavior of Ionic Liquid-Based Supercapacitors. *Batteries* **2024**, *10*, 266. <https://doi.org/10.3390/batteries10080266>

Academic Editor: Xin Chen

Received: 25 June 2024

Revised: 22 July 2024

Accepted: 24 July 2024

Published: 26 July 2024



**Copyright:** © 2024 by the authors. Licensee MDPI, Basel, Switzerland. This article is an open access article distributed under the terms and conditions of the Creative Commons Attribution (CC BY) license (<https://creativecommons.org/licenses/by/4.0/>).

**Keywords:** carbon-based supercapacitors; ionic liquids; acetonitrile; temperature influence; cycling stability

## 1. Introduction

Energy storage is crucial for managing the variable nature of renewable energy sources and meeting the energy needs of rapidly advancing electronic devices and electric transport [1]. Supercapacitors (SCs) have attracted considerable interest due to their high specific capacitance, rapid energy storage, and long cycle life [2]. The performance of electric double-layer capacitors (EDLCs) is influenced by how ions are distributed near the electrode surface. This sensitivity means that both the structure of the electrode pores and the composition of the electrolyte play crucial roles in determining their characteristics [3]. Additionally, the electrochemical stability window (ESW) is crucial as it limits energy density, emphasizing the need for electrolytes with wider electrochemical windows to design high-energy-density supercapacitors [4]. The ESW is influenced by the properties of ions and solvents, as well as interactions between ions, solvents, and the electrode–electrolyte interface [5]. Additionally, the purity of the electrolytes plays a substantial role in SC operation [6].

Ionic liquids (ILs) are organic salts with melting points below 100 °C, dissolving into free ions in a solvent. They are composed of an asymmetric organic cation combined with either an inorganic or organic anion. ILs offer high solubility, low volatility, a conductivity of 10<sup>-3</sup> to 10<sup>-2</sup> S·cm<sup>-1</sup>, and non-flammability, with benefits varying by cation–anion combination. Due to their unique properties, ILs are promising electrolytes for energy

storage devices [7]. Integrating ILs with nanostructured carbon could create advanced supercapacitors with high energy density and broad temperature range viability [8]. ILs have wider potential windows than water-based electrolytes, allowing higher energy densities despite higher viscosity. Strong ionic bonds also enhance stability and prevent evaporation.

ILs can be pure ILs, mixed, or quasi-solid-state electrolytes. Pure ILs are solvent-free, while mixtures improve energy storage potential. When selecting electrolytes, it is necessary to consider the support capabilities of the supercapacitor, such as ionic conductivity, thermal stability, operating voltage, specific energy, and power [9]. Using ILs alone is difficult due to high viscosity and cost. A practical approach involves integrating ILs into the electrolyte to improve ion mobility [10].

ILs are often combined with organic solvents to lower their viscosity and enhance the rate of ion transport [11], often quantified by the diffusion coefficient [12]. However, adding organic solvents reduces ionic association and alters the redox potential of ILs, narrowing the electrolyte's electrochemical stability window (ESW) and limiting the maximum working voltage (MWV) of EDLCs. The optimal concentration of ions and dissociation of ion pairs in IL-based electrolytes improve the mobility of cations and anions and ensure sufficient ion accessibility for charge transfer in carbon porous electrodes, resulting in the highest specific capacitance, with a tendency for it to increase with the MWV [13–15]. Consequently, pure ILs are preferred for achieving the highest energy density and specific capacitance in EDLCs. Nonetheless, when high-voltage devices are not required, a diluted IL electrolyte at an optimal concentration can be employed [16]. Adding organic solvents to ILs to diminish viscosity is an effective strategy for achieving desirable capacitive performance in EDLCs [17,18]. Acetonitrile (ACN), a common aprotic solvent, significantly enhances conductivity (up to 1.5 orders of magnitude) due to favorable interactions between ions and ACN, making conductivities less affected by the cation's size, shape, and mass [19]. Diluting ILs with AN generally boosts the ionic conductivity of a pure IL by improving ion transport rates (lower viscosity). Ionic conductivity is influenced by ionic density and the free volume of the electrolyte mixture [20,21].

ACN in EMIMBF<sub>4</sub> promotes ion solvation, reduces ion pairing, weakens Coulomb interactions, and facilitates ion mobility, thereby reducing IL viscosity [22,23]. The belief that lowering the electrolyte's viscosity enhances the specific capacitance is only valid when there are enough charge-carrying ions available. For example, graphene nanosheet electrodes demonstrate superior capacitive performance in a 2.0 M EMIMBF<sub>4</sub>/acetonitrile electrolyte, featuring a wide voltage window (2.3 V), minimal infrared drop, and high specific capacitance (128.2 F g<sup>-1</sup>) [24]. However, studies on the optimal IL concentration are lacking, and further studies are needed to enable the practical application of IL solvent electrolytes [4].

The practical application of ILs in energy storage systems requires an understanding of the electrolyte's physical properties at various temperatures, which significantly affect their viscosity and ionic conductivity and hence their long-term cycle life [25,26]. Therefore, understanding the temperature dependence for a specific IL-electrolyte system is crucial. For instance, it has been observed that a supercapacitor using the EMIMBF<sub>4</sub>/acetonitrile electrolyte demonstrates long-term cyclic stability in charge/discharge cycles at both low and high operating temperatures for up to 1500 cycles. Beyond this point, galvanostatic charge/discharge curves noticeably deviate from ideal symmetric forms, leading to a significant decrease in specific capacitance [27].

In the present work, the electrochemical performance of symmetric activated carbon-based supercapacitors with EMIMBF<sub>4</sub> ionic liquid-based electrolytes and different ACN ratios were investigated through long-term galvanostatic charge/discharge tests, impedance studies, and cyclic voltammetry at different heating modes from 24 to 60 °C. In order to clarify the reasons for the ongoing processes in the investigated systems, electrochemical studies were also carried out after the prolonged regimes.

## 2. Materials and Methods

### 2.1. Electrolyte Preparation

The electrolyte contained a neat ionic liquid (1-Ethyl-3-methylimidazolium tetrafluoroborate, Fluorochem 96.3% (HPLC)) and mixtures of ionic liquid and acetonitrile (Spectrophotometric Grade, 99.7+% Alfa Aesar) in various vol.% ratios: EMIMBF<sub>4</sub>:ACN = 9:1 (9IL/ACN), EMIMBF<sub>4</sub>:ACN = 2:1 (2IL/ACN), EMIMBF<sub>4</sub>:ACN = 1:1 (IL/ACN), and EMIMBF<sub>4</sub>:ACN = 1:2 (IL/2ACN). For comparison, neat ACN was also examined.

The electrolytes were prepared in a glove box mBraun-Labmaster Pro.

### 2.2. Preparation of the Carbon Electrodes and Supercapacitor Cell Assembly

Commercial activated carbon (YP-50F, “Kuraray Europe” GmbH) was used as the active material to prepare the electrodes for supercapacitor cells. The composition consisted of 80 wt.% activated carbon, 10 wt.% poly(vinylidene fluoride-co-hexafluoropropylene), and 10 wt.% graphite fibers.

Before use, the binder poly(vinylidene fluoride-co-hexafluoropropylene, Sigma-Aldrich, St. Louis, MI, USA) in the form of granules was dissolved in N,N-dimethylacetamide (3% solution, 99% Alfa Aesar), to obtain a homogeneous mixture. All materials were stirred for 15 min.

The electrode layers were prepared using a casting technique. This involved pouring the electrode mixture onto a glass plate, followed by several drying stages: 5 h at 40 °C to evaporate the solvent, then drying for 12 h at 70 °C. The forming free-standing flexible film electrode was detached with distilled water and thermally treated at 120 °C for 1 h to remove the traces of water, and then finally heated for 20 min at 160 °C to improve the mechanical strength [28].

Before assembly, the electrodes were cut with a circular area of 0.64 cm<sup>2</sup>, dried under a vacuum at 80 °C for 12 h in order to outgas the electrode, and then mounted in a two-electrode coin Swagelok-type cell with a Whatman separator. The cell was filled with the electrolyte in a dry box under an argon atmosphere (H<sub>2</sub>O and O<sub>2</sub> < 0.01 ppm).

### 2.3. Electrochemical Characterization

The performance of the supercapacitors was investigated through a series of electrochemical measurements using cyclic voltammetry (CV) at different scan rates ranging from 10 to 50 mVs<sup>-1</sup>, within a voltage range of 0.05–3.2 V, depending on the electrolyte composition. These measurements were conducted using a Multi PalmSens system (model 4, Houten, The Netherlands). Electrochemical impedance spectroscopy (EIS) investigations were performed using the same apparatus, with frequencies ranging from 10 MHz to 1 mHz.

Cyclic galvanostatic charge–discharge (GCD) and long-term tests were performed using an Arbin LBT21084 measurement system. The GCD tests were conducted over the voltage range of 0.05–2.8 V and 0.05–3.0 V while continuously charging the cells with a current of 200 to 4000 mAg<sup>-1</sup> for 100 cycles per step. Long-term tests were carried out for 5000 charge and discharge cycles at 200 mAg<sup>-1</sup>.

The specific capacitance determined from the cyclic voltammetry curves is calculated using Equation (1) and the specific capacitance is calculated from the charge/discharge curves according to Equation (2):

$$C_s = [4(I/(dV/dt))/m] \quad (1)$$

where dV/dt is the voltage scan rate, I is the current, and m is the mass of the active carbon material.

$$C = [4(I \times \Delta t)/(m \times \Delta V)] \quad (2)$$

where  $\Delta t$  (s), m (g),  $\Delta V$  (V), and I (A) indicate the discharge time, mass of active material, voltage window, and discharge current, respectively. The value 4 is necessary to denote the capacitance of a single electrode [28].

The energy density ( $E$ ) and power density ( $P$ ) are calculated from Equations (3) and (4), using the specific discharge capacitance:

$$E = C \Delta V^2 / 7.2 \quad (3)$$

and

$$P = 3600 E/t \quad (4)$$

### 3. Results and Discussion

The different characteristics of ILs necessitate careful selection based on the specific operating conditions and requirements of the device being developed. Additionally, the structure of electrodes affects how ionic liquids (ILs) are arranged at the interface. Mixing ILs with organic electrolytes can enhance conductivity and durability under harsh conditions. However, this method narrows the voltage window of IL electrolytes, which in turn limits the energy density of supercapacitors [8].

Conductivity and viscosity are key parameters that significantly influence electrolyte characteristics. Establishing a relationship between these parameters and molar concentration is crucial, especially for ionic liquids due to their high viscosity. Although partial data exist for some systems, comprehensive studies aimed at determining the optimal concentration of ionic liquids are still lacking [19]. In this study, a pure electrolyte of EMIMBF<sub>4</sub> and its mixtures with ACN in various volume ratios were investigated. EMIMBF<sub>4</sub> was selected because it is one of the most commonly used ionic liquids in experimental studies on supercapacitors [29] and offers high electrochemical stability [30]. On the other hand, acetonitrile was chosen as the organic solvent due to its outstanding oxidative stability and high dielectric constant, which ensures its compatibility with electrolyte salts. [31]. ACN has a much lower viscosity compared to EMIMBF<sub>4</sub> (0.3 centipoises versus 41 centipoises, respectively), which is likely to reduce charge transfer resistance and consequently improve the rate performance of the SC [32].

Various methods have been employed to accurately investigate the electrochemical characteristics of SCs with different ACN ratios. To monitor changes in the investigated systems, CV and EIS curves were recorded at the beginning of the experiments and after conducting a long-term galvanostatic charge/discharge test. The resulting CV curves, recorded at 10 mVs<sup>-1</sup> and different voltage windows, are presented in Figure 1. For comparison, the voltammograms of pure ACN are also presented.

The initial voltammograms exhibit the typical characteristics of symmetrical supercapacitor systems. Supercapacitors with IL electrolytes containing ACN show nearly rectangular shapes, unlike those using pure EMIMBF<sub>4</sub>. This difference can be explained by the lower resistance in the supercapacitor due to the reduced viscosity of the electrolyte. This result is expected and is most likely due to the reduced ionic association that occurs when organic solvents are introduced into pure IL. This change alters the redox potential, resulting in a narrowing of the electrochemical stability window of the electrolyte. Although the potential window does not reach the electrolyte's decomposition voltage, local high voltages in porous carbon can cause decomposition. Additionally, the strong polarity of ionic liquids makes it difficult to eliminate trace water, which may also lead to electrolyte decomposition and affect the potential window [33].

Galvanostatic charge/discharge tests were conducted at different current loads and long-term studies were performed. Based on the results shown in Figure 1, the voltage limits for the investigated supercapacitors were selected, ensuring that the electrolyte remained stable and its efficiency and longevity were not compromised by undesirable chemical reactions. The voltage limits were set at 0.05–3.0 V for neat IL and the electrolyte mixture containing a small amount of 9IL/ACN, and at 0.05–2.8 V for the other studied solutions.

A significant drawback of ionic liquids is their low stability during prolonged cycling, which has focused our efforts on conducting long-term tests. The results of these tests at a current load of 200 mA g<sup>-1</sup> for a total of 5000 cycles are shown in Figure 2.

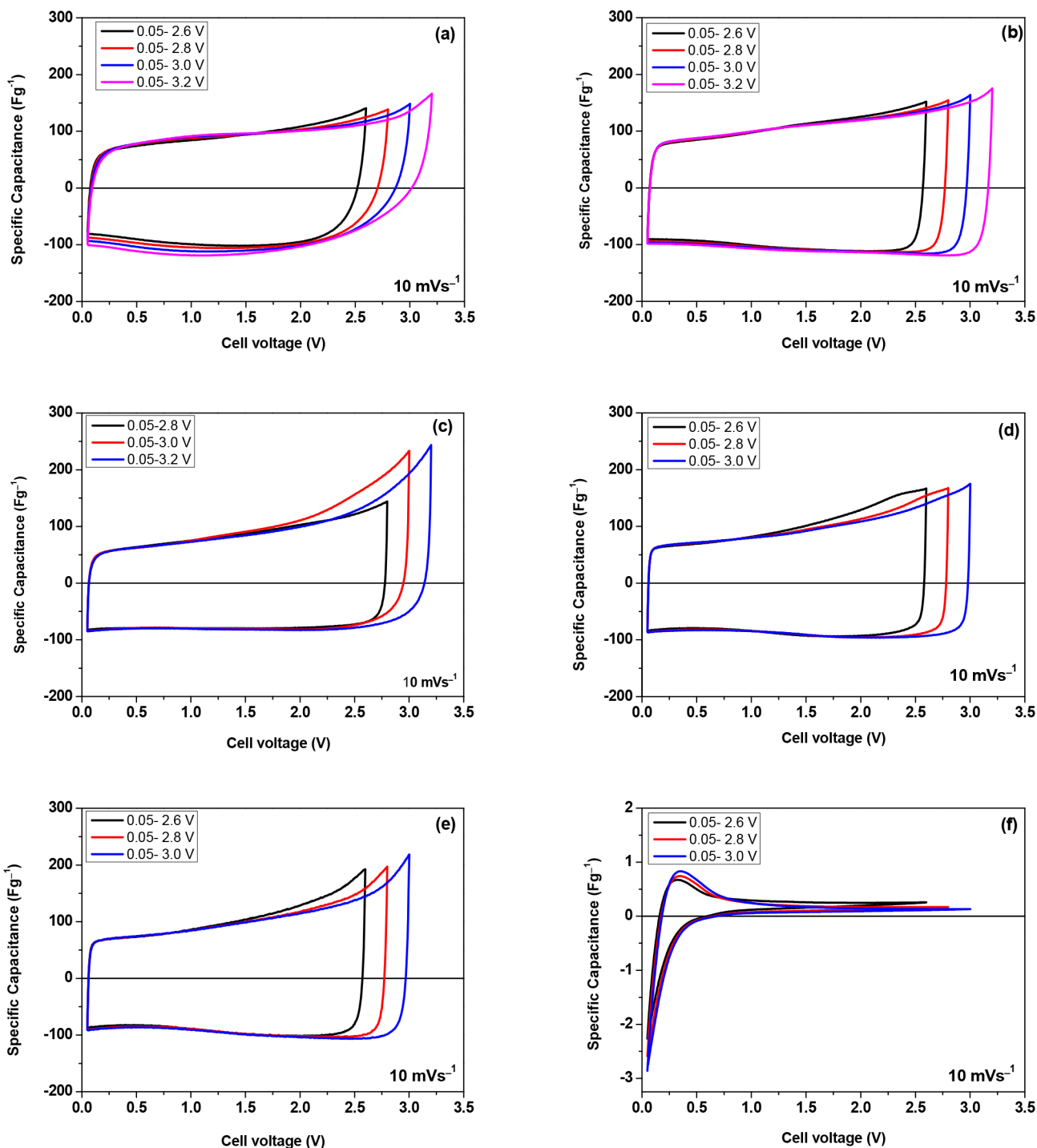


**Figure 1.** Cyclic voltammogram curves measured at a scan rate of  $10 \text{ mVs}^{-1}$  at different voltage ranges from 0.05 to 3.2 V for symmetric supercapacitors with varying ratios of ACN to EMIMBF<sub>4</sub>: IL: (a), 9IL/ACN (b), IL/ACN (c), 2IL/ACN (d), IL/2ACN (e), and ACN (f).

The results show that increasing the concentration of ions in pure ionic liquids (ILs) does not significantly enhance the capacitance of nanoporous carbon-based EDLCs. This is due to the increased difficulty in separating ions with opposite charges in pure ILs. The mechanism of EDLCs changes from the adsorption of opposite ions in dilute ACN to an ion exchange in pure ILs. Furthermore, the interface structure is influenced by both the electrode surface and the IL electrolytes [34].

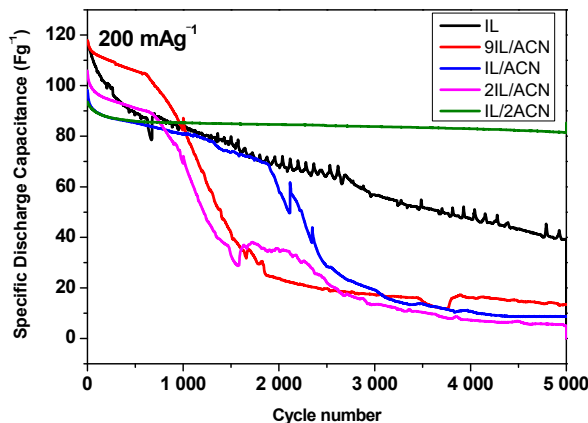


**Figure 2.** Long-term cycling stability at  $200 \text{ mAg}^{-1}$  of the symmetrical supercapacitors with different electrolyte ratios of ACN to  $\text{EMIMBF}_4$  up to 5000 GCD cycles.

A detailed look of the cyclic stability curves reveals distinct electrochemical characteristics. Up to 1000 cycles, the discharge capacitance of the SC with pure ionic liquid is the highest, but it has low stability, reaching a value of 65% loss at 5000 cycles. After 1000 cycles, a sharp decline in the stability of the SC with electrolytes is observed, where the IL/ACN ratio favors IL. By 1900 charge/discharge cycles, similar behavior is noted with the SC using electrolytes containing IL/ACN. An impressive result, however, is observed with the cyclic stability of the SC with IL/2ACN. The discharge capacitance remains nearly constant, with capacitance loss not exceeding 13% after 5000 cycles. In order to clarify the results obtained, paying particular attention to the increased stability upon cycling of the SC with electrolytes containing IL/2ACN, CV curves were also performed after prolonged cycling (Figure 3a,b), as well as impedance measurements. In addition, voltage profiles before and after cycling tests at  $200 \text{ mAg}^{-1}$  are presented in Figure 3c,d, which aids in the overall analysis of the results.

For a better understanding of the long-term test results, Table 1 presents the calculated values for the discharge capacitance retention after 5000 cycles and for the ohmic drop before and after the GCD test.

**Table 1.** Capacitance retention after 5000 charge/discharge cycles and ohmic drops before and after cycling.

Electrolyte Composition, IL:AN	Capacitance Retention after 5000 GDC, %	iR Drops—Initial, V	iR Drops—after 5000 GDC, V
IL	33	0.087	0.452
9IL/ACN	12	0.025	1.101
2IL/ACN	5	0.021	1.943
IL/ACN	9	0.019	1.975
IL/2ACN	87	0.016	0.082

The results in Table 1 show that during the first cycle, the ohmic drop of the cell with pure IL is the highest. As the ACN content in the electrolyte increases, the ohmic drop in the cell decreases. Considering that the ‘IR drop’ includes the resistance of the electrolyte solution, the contact resistance at the interface between the active material and the receiver, and the internal resistance of the active material, with the electrolyte solution’s resistance usually being predominant, the results obtained are probably related to an increase in the electrolyte’s conductivity, as impedance studies have shown [35]. However, after 5000 cycles, the cell with a 2:1 ratio exhibits the lowest ohmic drop and maintains almost constant capacitance (only a 13% decrease). For the other cells, the ohmic drop increases significantly, leading to a sharp decline in their discharge capacitance. A possible reason

for this is the degradation of the electrolyte and the formation of a passivation layer on the electrodes, as discussed by K. Karuppasamy et al. [33].

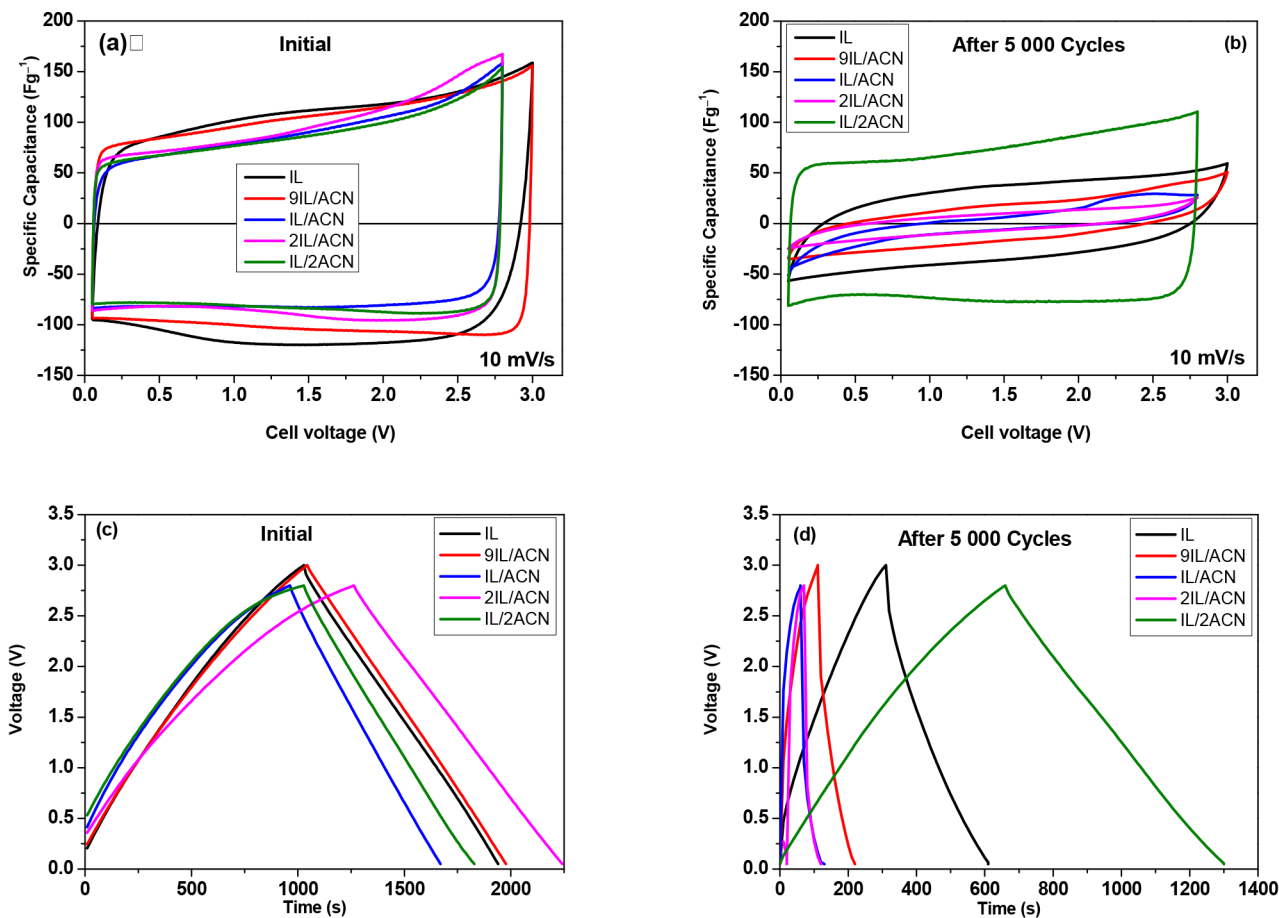


**Figure 3.** Cyclic voltammograms at scan rate of  $10 \text{ mV s}^{-1}$  (a,b) and galvanostatic charge/discharge curves at  $200 \text{ mA g}^{-1}$  (c,d) for symmetric SCs before and after 5000 GCD cycles.

As can be seen, the rectangular shape of the IL/2ACN supercapacitor remains unchanged, with area shrinkage observed. This result confirms the good stability of this supercapacitor. Conversely, the shape of the CV curves in other investigated systems changes, which is in agreement with the results of the long-term galvanostatic test (Figure 3).

The electrochemical properties of the studied carbons were assessed using Ragon plots for supercapacitor cells with different electrolyte compositions before and after the long-term test (Figure 4).

The energy density of the SCs before the start of the long-term test was highest for SCs with pure ionic liquid and those with an electrolyte containing acetonitrile in an IL/ACN ratio of 9:1 (35 and 36 Wh kg<sup>-1</sup> at power outputs of 140 and 137 W kg<sup>-1</sup>, respectively). However, after 5000 charge/discharge cycles at  $200 \text{ mA g}^{-1}$ , the trend changes. The SC with an electrolyte containing an IL/ACN ratio of 1:2 shows the highest energy density (21 Wh kg<sup>-1</sup> at a power output of 120 W kg<sup>-1</sup>), while the energy density of the SC with pure ionic liquid decreases drastically (12 Wh kg<sup>-1</sup> at a power output of 141 W kg<sup>-1</sup>), even with a wider voltage window.

Rate response is a crucial performance parameter for electric double-layer capacitors, evaluated by charging and discharging them at different current densities. The discharge capacitance and their dependence on the current rate were compared for the supercapacitor showing the most stable behavior in an electrolyte with IL/2ACN, and for the SC with an electrolyte containing neat IL (Figure 5).

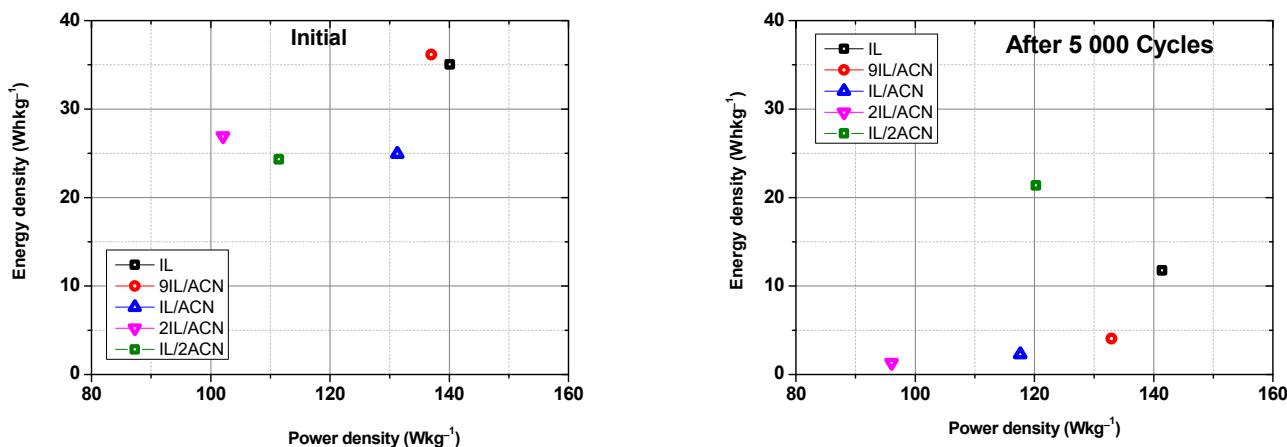


**Figure 4.** Energy density versus power density (Ragone plot) for symmetric supercapacitors with different IL electrolyte compositions.

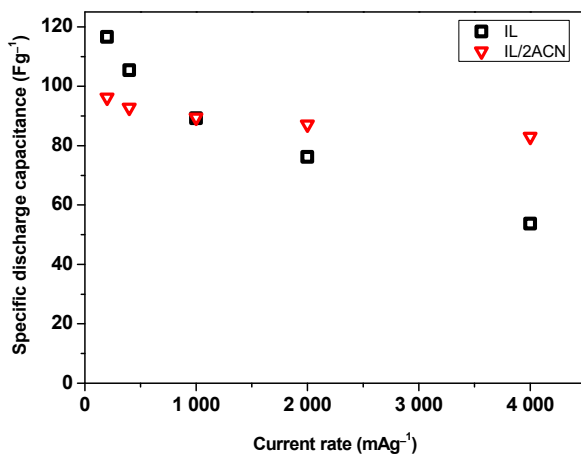


**Figure 5.** Specific discharge capacitance as a function of current load for symmetric supercapacitors with electrolytes containing IL and IL/2ACN.

As shown in Figure 5, the SC using IL/2ACN has the most stable behavior, maintaining a constant discharge capacity at different current rates. Conversely, the SC with pure EMIMBF<sub>4</sub> shows a noticeable drop in capacitance with the increasing current load. These findings indicate that the IL/2ACN electrolyte improves the rate response in terms of rate, providing more reliable operation under different discharge conditions. This improvement can be attributed to the significant influence of electrolyte viscosity and conductivity on the rate response.

Figure 5 demonstrates that the supercapacitor (SC) utilizing IL/2ACN exhibits the most stable behavior, maintaining a consistent discharge capacitance across various current rates. In contrast, the SC employing pure EMIMBF<sub>4</sub> experiences a notable decline in capacitance as the current load increases. These observations suggest that the IL/2ACN electrolyte enhances the rate response, ensuring more dependable operation under diverse discharge conditions. This enhancement is attributed to the considerable impact of electrolyte viscosity and conductivity on the rate response. This trend is reflected in the Ragone plot (Figure 6), illustrating a slight reduction in energy density (from 25.5 to 21.5 Wh kg<sup>-1</sup>) with increasing power density (from 138 to 2750 W kg<sup>-1</sup>) for the IL/2ACN SC.

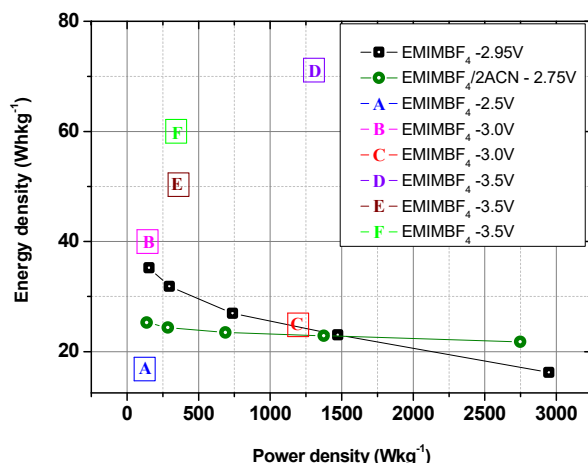


**Figure 6.** Energy density versus power density (Ragone plot) for symmetric supercapacitors with  $\text{EMIMBF}_4:\text{ACN} = 1:2$  (IL/2ACN). The literature data for carbon-based SCs with neat  $\text{EMIMBF}_4$  are presented for comparison: A [36], B [37], C [38], D [39], E [40], F [41].

The study of supercapacitors using ionic liquids at elevated temperatures is of major importance due to their distinctive chemical composition and characteristics. ILs are more viscous than conventional electrolytes due to the large size of the ions, resulting in reduced capacitance and power density at room temperature. However, studies have shown that optimal IL performance is achieved at temperatures around  $60\text{ }^\circ\text{C}$  [42]. Furthermore, temperature has a significant impact on both the lifetime estimation and the efficiency enhancement of the supercapacitor [24].

Our studies at elevated temperatures ( $40$  and  $60\text{ }^\circ\text{C}$ ) were mainly focused on the investigation of supercapacitors with neat ionic liquid and with the IL/2ACN electrolyte, which showed the highest cycling stability at room temperature. The results are presented in Figures 7 and 8 and show that the SC with the IL/2ACN electrolyte has a stable behavior at  $40\text{ }^\circ\text{C}$ .

Electrochemical impedance spectroscopy (EIS) was performed to analyze the impedance characteristics with different ratios of ACN in the electrolyte, both at the beginning of the tests and after 5000 cycles. Figure 9 presents the Nyquist plot and the capacitance versus frequency dependence, while Table 2 shows the calculated values.

**Table 2.** The values of electrolyte resistance ( $\text{Rel}$ ), electrode resistance ( $\text{Rp}$ ), and cell resistance ( $\text{Ri}$ ) determined from Nyquist plots.

Electrolyte Composition, IL/AN	Temperature	$\text{Rel}$ $\Omega$	$\text{Rp}$ $\Omega$	$\text{Ri}$ $\Omega$
IL	room temperature	2.2	2.3	11.5
	after 5000 cycles	6.8	-	52
	$40\text{ }^\circ\text{C}$	1.7	3.7	8.9
	$60\text{ }^\circ\text{C}$	1.3	3.3	6.78
IL/2ACN	room temperature	1.13	0.35	3.2
	after 5000 cycles	1.7	0.9	6.2
	$40\text{ }^\circ\text{C}$	1.02	0.53	2.9
	$60\text{ }^\circ\text{C}$	0.94	0.48	-

The Nyquist plots are inherent to the porous electrodes in the carbon bilayer capacitors. The semicircle at high frequencies is due to the pore resistance/resistance of the electrodes ( $\text{Rp}$  is the diameter of the semicircle), the line with a slope  $\leq 45^\circ$  at medium to low frequencies is due to the diffuse region, and the nearly vertical line at low frequencies is the capacitive part is due to the capacitance of DL. From the intersection of its continuation with  $Z'$ , the cell resistance ( $\text{Ri}$ ) is determined. The left intercept of  $Z''$  at the  $Z'$  axis (the

origin of the semicircle) represents the resistance ( $R_{el}$ ) of the electrolyte in the cell. As can be seen from Table 2 the addition of ACN causes a decrease in  $R_i$ . The same role is played by the increase in operating temperatures as can be seen from the Nyquist plots of SCs with IL and IL/2ACN (Figure 10). In both cases, the decrease in  $R_i$  is a result of a decrease in  $R_{el}$  and a shortening of the diffuse portion (i.e., a decrease in diffusion resistance).

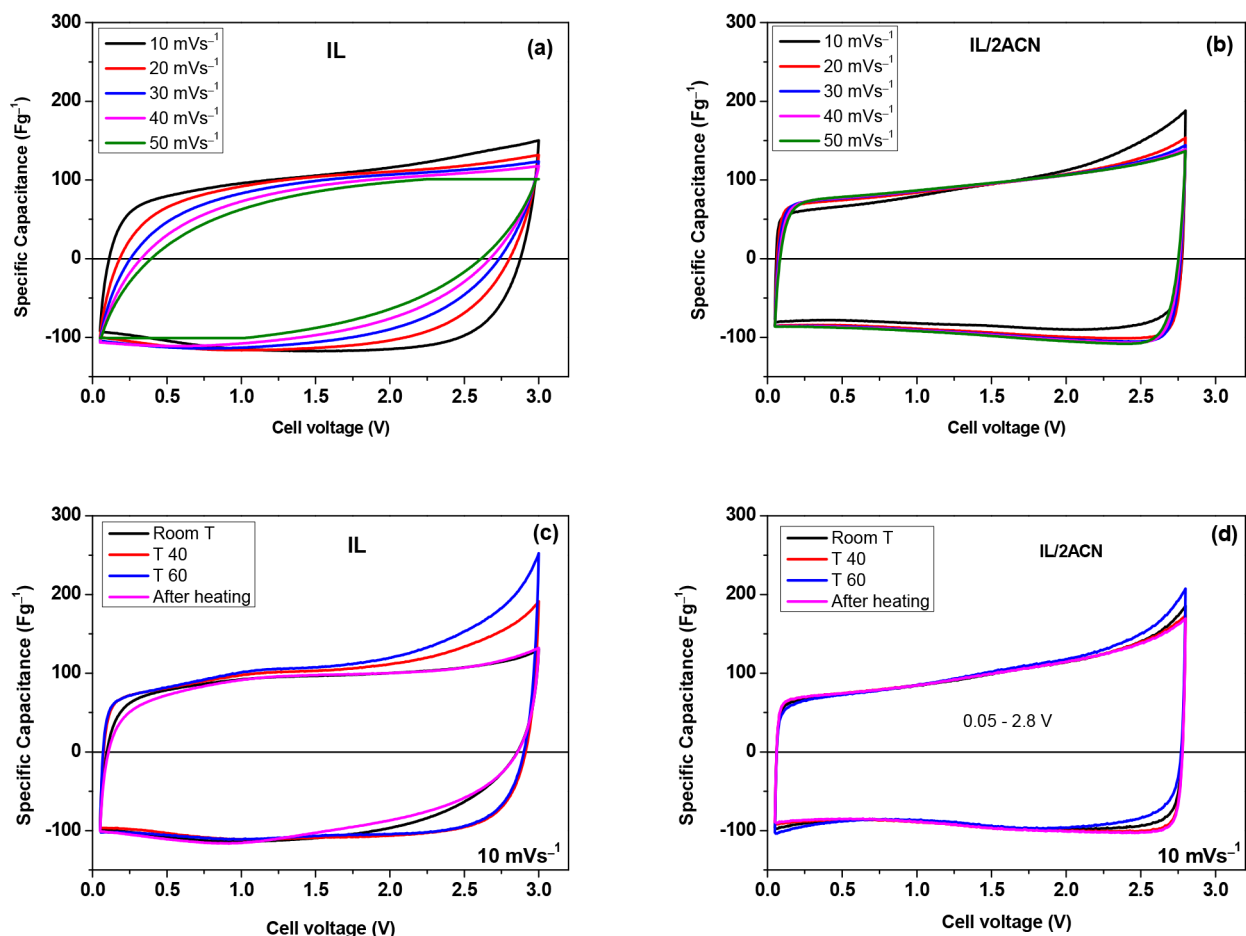


**Figure 7.** Cyclic voltammograms for SCs with IL and IL/2ACN electrolyte at room temperature and different scan rates (a,b) and at scan rates of  $10 \text{ mV s}^{-1}$  and  $40^\circ\text{C}$  and  $60^\circ\text{C}$  (c,d).

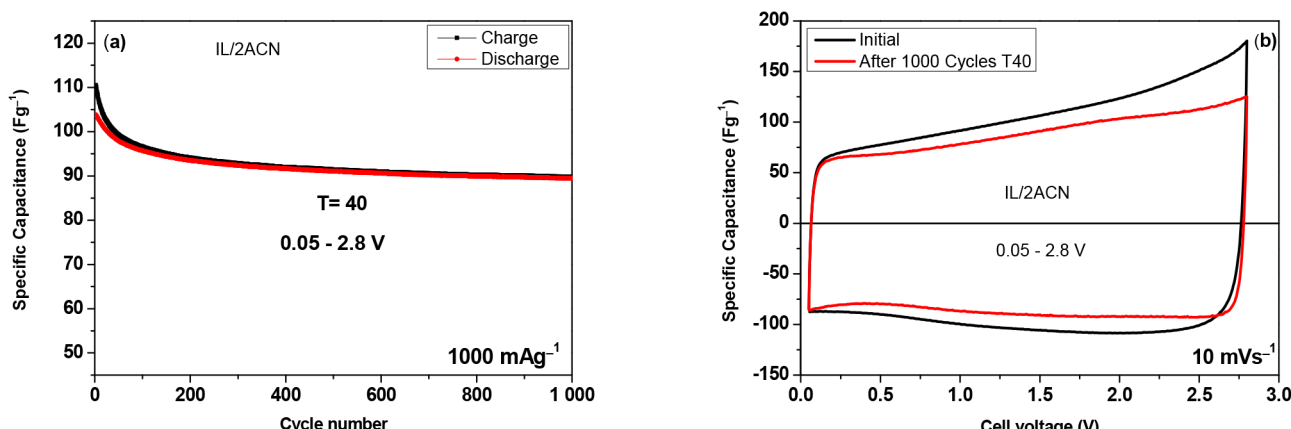


**Figure 8.** Long-term cycling stability at  $1000 \text{ mAg}^{-1}$  of the symmetrical supercapacitor with the IL/2ACN electrolyte (a) and cyclic voltammograms before and after 1000 GCD cycles (b).

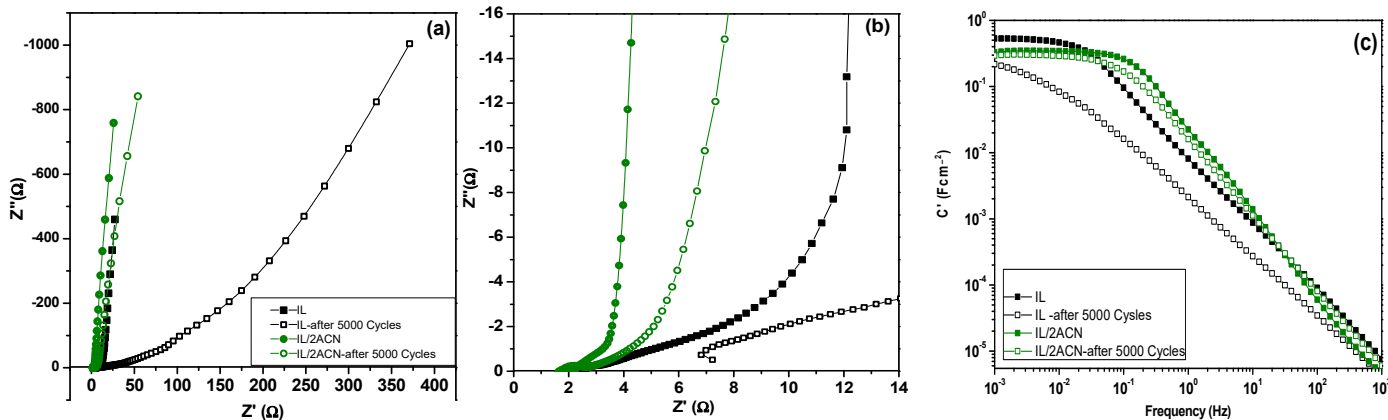


**Figure 9.** EIS of SCs with neat EMIMBF<sub>4</sub> and IL/2ACN initially and after 5000 GCD: Nyquist plots (a) full scale and (b) zoomed; C' vs. frequency of the cells (c).

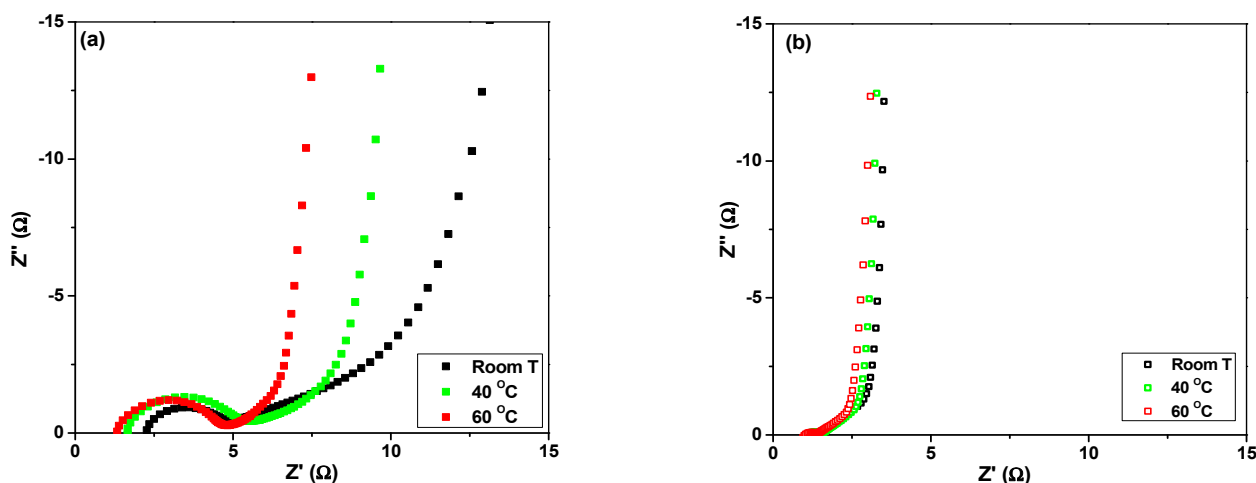


**Figure 10.** Nyquist plots of SCs with IL (a) and IL/2ACN (b) at different temperatures.

The addition of ACN has a contradictory effect on the stability of the cell under cycling. In relatively small amounts, prolonged cycling leads to a decrease in Rel and a change in the nature of the AC response, namely from capacitive to diffusive (Figures 9b and 10). At a ratio of 1:2, the increase in  $R_i$  is small, the capacitive character is preserved, and the capacitance is close to the initial sample. Our assumption of good stability is that with enough ACN, it plays a dual role—on the one hand, the viscosity decreases sharply, thereby facilitating ion transport, and on the other hand, it prevents IL degradation.

Additional information can be obtained from the diffusion coefficient ( $D$ ), which can be calculated using Equations (5) and (6) that are valid in the diffusion region [43–45]:

$$-Z'' = \frac{1}{C_l \omega'} \quad (5)$$

and

$$IZI = \frac{L}{C_l (D \omega)^{-1/2}} \quad (6)$$

where  $L$  and  $C_l$  are the thickness and capacitance, respectively.

Therefore,  $C_l$  and  $D$  can be calculated from the slopes of the  $-Z''$  vs.  $\omega^{-1}$  and  $IZI$  vs.  $\omega^{-1/2}$  linear plots, as illustrated in Figure 11, while Table 3 presents the calculated values.

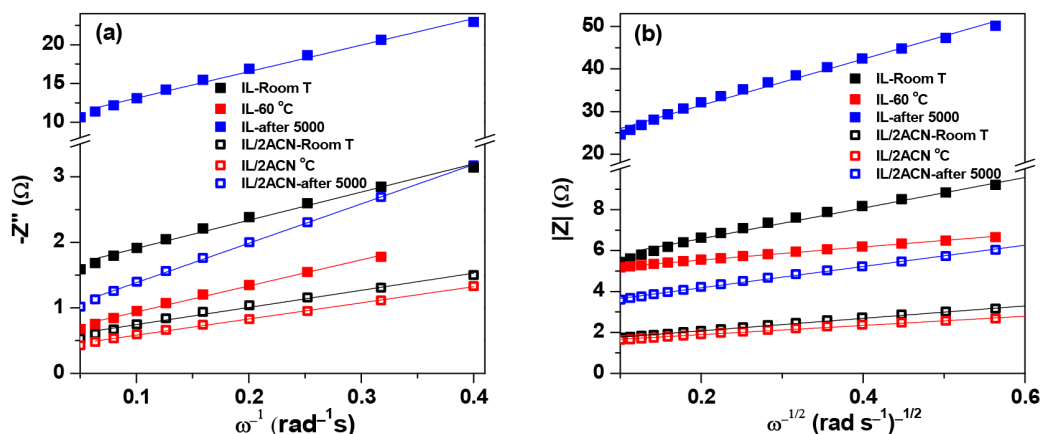


**Figure 11.** Plots of  $-Z''$  vs.  $\omega^{-1}$  (a) and  $IZI$  vs.  $\omega^{-1/2}$  (b) for diffusion coefficient determination.

**Table 3.** Calculated values of diffusion coefficient ( $D$ ) of pure IL and IL/2AN at different temperatures.

Electrolyte Composition, IL/AN	Temperature	$D$ $\text{m}^2\text{s}^{-1}$
IL	room temperature	$7.01 \times 10^{-8}$
	after 5000 cycles	$1.05 \times 10^{-7}$
	60 °C	$3.85 \times 10^{-7}$
IL/2ACN	room temperature	$1.06 \times 10^{-7}$
	after 5000 cycles	$1.64 \times 10^{-7}$
	60 °C	$2.38 \times 10^{-7}$

The resulting values for  $D$  correlate with those reported by [46]. No decrease in the value of the diffusion coefficient of pure IL was observed after 5000 charge/discharge cycles despite the deteriorated cell characteristics. This is a surprising result that deserves further investigation.

#### 4. Conclusions

Studies on symmetric supercapacitors using an EMIMBF<sub>4</sub>-based electrolyte with various ratios of acetonitrile (ACN) demonstrate that adding ACN significantly enhances electrochemical stability and reduces internal resistance. These improvements are due to ACN's dual role at higher concentrations: it significantly lowers viscosity, facilitates ion transport, and prevents the degradation of the ionic liquid (IL). Optimal performance is observed at a volumetric ratio of 1:2 for EMIMBF<sub>4</sub> to ACN. The supercapacitor shows 87% cyclic stability over 5000 charge/discharge cycles within a voltage range of 0.05–2.8 V and at a current density of 1 A g<sup>-1</sup>, achieving an energy density of 23 Wh kg<sup>-1</sup> and a power density of 748 W kg<sup>-1</sup>. Moreover, these supercapacitors exhibit stability at elevated temperatures up to 60 °C, showing no degradation under varying thermal conditions.

Adding solvents such as ACN to EMIMBF<sub>4</sub> is a practical approach to reduce costs in IL-supercapacitors, which are promising due to their relatively high energy density and power characteristics. These findings provide a basis for future research aimed at developing more efficient solutions using compatible and environmentally friendly materials to produce safe, efficient, and reliable IL-based devices capable of operating under a variety of conditions.

**Author Contributions:** Conceptualization, A.S. and T.S.; methodology, A.S., T.S. and B.K.; validation, B.K. and L.S.; investigation, B.K. and L.S.; data curation, B.K., E.L. and L.S.; writing—original draft preparation, B.K. and T.S.; writing—review and editing, A.S. and E.L.; visualization, B.K.; project administration, B.K.; funding acquisition, B.K. All authors have read and agreed to the published version of the manuscript.

**Funding:** This research was funded by the Bulgarian Ministry of Education and Science under the National Program “Young Scientists and Postdoctoral Students-2”.

**Data Availability Statement:** The original contributions presented in the study are included in the article.

**Acknowledgments:** The authors gratefully acknowledge the support of the Bulgarian Ministry of Education and Science under the National Program “Young Scientists and Postdoctoral Students-2”.

**Conflicts of Interest:** The authors declare no conflicts of interest. The funders had no role in the design of the study; in the collection, analyses, or interpretation of the data; in the writing of the manuscript; or in the decision to publish the results.

## References

1. González, A.; Goikolea, E.; Barrena, J.A.; Mysyk, R. Review on supercapacitors: Technologies and materials. *Renew. Sustain. Energy Rev.* **2016**, *58*, 1189–1206. [[CrossRef](#)]
2. Czagany, M.; Hompoth, S.; Keshri, A.K.; Pandit, N.; Galambos, I.; Gacs, Z.; Baumli, P. Supercapacitors: An Efficient Way for Energy Storage Application. *Materials* **2024**, *17*, 702. [[CrossRef](#)]
3. Liu, K.; Wu, J. Boosting the Performance of Ionic-Liquid-Based Supercapacitors with Polar Additives. *J. Phys. Chem. C* **2016**, *120*, 24041–24047. [[CrossRef](#)]
4. Wang, Y.; Xue, K.; Yan, C.; Li, Y.; Zhang, X.; Su, K.; Ma, P.; Wan, S.; Lang, J. Tuning of Ionic Liquid–Solvent Electrolytes for High-Voltage Electrochemical Double Layer Capacitors: A Review. *Batteries* **2024**, *10*, 54. [[CrossRef](#)]
5. Venâncio, R.; Vicentini, R.; Pinzón, C.M.J.; Corrêa, D.A.; Miranda, A.N.; Queiroz, A.C.; Degasperi, F.T.; Siqueira, L.J.; Da Silva, L.M.; Zanin, H. Combining electrochemical, molecular simulation and operando techniques to investigate the stability of electrodes and organic electrolytes used in EDLCs. *Energy Storage Mater.* **2023**, *62*, 102943. [[CrossRef](#)]
6. Mendhe, A.; Panda, H.S. A review on electrolytes for supercapacitor device. *Discov. Mater.* **2023**, *3*, 29. [[CrossRef](#)]
7. Xiong, W.; Yin, Z.; Zhang, X.; Tu, Z.; Hu, X.; Wu, Y. Ionic Liquids Endowed with Novel Hybrid Anions for Supercapacitors. *ACS Omega* **2022**, *7*, 26368–26374. [[CrossRef](#)]
8. Pan, S.; Yao, M.; Zhang, J.; Li, B.; Xing, C.; Song, X.; Su, P.; Zhang, H. Recognition of Ionic Liquids as High-Voltage Electrolytes for Supercapacitors. *Front. Chem.* **2020**, *8*, 261. [[CrossRef](#)]
9. Rahmi, V.A.; Zunita, M. Ionic liquid-based electrolyte in supercapacitors. *AIP Conf. Proc.* **2024**, *3073*, 060001. [[CrossRef](#)]
10. Eftekhari, A. Supercapacitors utilising ionic liquids. *Energy Storage Mater.* **2017**, *9*, 47–69. [[CrossRef](#)]
11. Chaban, V.V.; Voroshyllova, I.V.; Kalugin, O.N.; Prezhdo, O.V. Acetonitrile Boosts Conductivity of Imidazolium Ionic Liquids. *J. Phys. Chem. B* **2012**, *116*, 7719–7727. [[CrossRef](#)]
12. Yang, H.; Yang, J.; Bo, Z.; Chen, X.; Shuai, X.; Kong, J.; Yan, J.; Cen, K. Kinetic-Dominated Charging Mechanism within Representative Aqueous Electrolyte-based Electric Double-Layer Capacitors. *J. Phys. Chem. Lett.* **2017**, *8*, 3703–3710. [[CrossRef](#)]
13. Wu, G.; Tan, P.; Wang, D.; Li, Z.; Peng, L.; Hu, Y.; Wang, C.; Zhu, W.; Chen, S.; Chen, W. High-performance Supercapacitors Based on Electrochemical-induced Vertical-aligned Carbon Nanotubes and Polyaniline Nanocomposite Electrodes. *Sci. Rep.* **2017**, *7*, 43676. [[CrossRef](#)]
14. Yu, C.; Masarapu, C.; Rong, J.; Wei, B.; Jiang, H. Stretchable Supercapacitors Based on Buckled Single-Walled Carbon-Nanotube Macrofilms. *Adv. Mater.* **2009**, *21*, 4793–4797. [[CrossRef](#)]
15. Lei, Z.; Liu, Z.; Wang, H.; Sun, X.; Lu, L.; Zhao, X.S. A high-energy-density supercapacitor with graphene–CMK-5 as the electrode and ionic liquid as the electrolyte. *J. Mater. Chem. A* **2013**, *1*, 2313–2321. [[CrossRef](#)]
16. Wong, S.I.; Lin, H.; Sunarso, J.; Wong, B.T.; Jia, B. Optimization of ionic-liquid based electrolyte concentration for high-energy density graphene supercapacitors. *Appl. Mater. Today* **2020**, *18*, 100522. [[CrossRef](#)]
17. Frackowiak, E. Supercapacitors based on carbon materials and ionic liquids. *J. Braz. Chem. Soc.* **2006**, *17*, 1074–1082. [[CrossRef](#)]
18. Zhang, S.; Brahim, S.; Maat, S. High-voltage operation of binder-free CNT supercapacitors using ionic liquid electrolytes. *J. Mater. Res.* **2018**, *33*, 1179–1188. [[CrossRef](#)]
19. Chaban, V.V.; Voroshyllova, I.V.; Kalugin, O.N.; Prezhdo, O.V. Acetonitrile Drastically Boosts Conductivity of Ionic Liquids. *arXiv* **2012**. [[CrossRef](#)]
20. Wang, H.; Liu, S.; Huang, K.; Yin, X.; Liu, Y.; Peng, S. BMIMBF<sub>4</sub> Ionic Liquid Mixtures Electrolyte for Li-ion Batteries. *Int. J. Electrochem. Sci.* **2012**, *7*, 1688–1698. [[CrossRef](#)]
21. Kwon, H.-N.; Jang, S.-J.; Kang, Y.C.; Roh, K.C. The effect of ILs as co-salts in electrolytes for high voltage supercapacitors. *Sci. Rep.* **2019**, *9*, 1180. [[CrossRef](#)]
22. Ruiz, V.; Huynh, T.; Sivakkumar, S.R.; Pandolfo, A.G. Ionic liquid–solvent mixtures as supercapacitor electrolytes for extreme temperature operation. *RSC Adv.* **2012**, *2*, 5591–5598. [[CrossRef](#)]
23. Deshpande, A.; Kariyawasam, L.; Dutta, P.; Banerjee, S. Enhancement of Lithium Ion Mobility in Ionic Liquid Electrolytes in Presence of Additives. *J. Phys. Chem. C* **2013**, *117*, 25343–25351. [[CrossRef](#)]
24. Liu, W.; Yan, X.; Lang, J.; Xue, Q. Effects of concentration and temperature of EMIMBF<sub>4</sub>/acetonitrile electrolyte on the supercapacitive behavior of graphene nanosheets. *J. Mater. Chem.* **2012**, *22*, 8853–8861. [[CrossRef](#)]

25. Bahaa, A.; Alhammadi, A.; Lethesh, K.C.; Susantyoko, R.A.; Bamgbopa, M.O. Ionic liquid electrolyte selection for high voltage supercapacitors in high-temperature applications. *Front. Chem.* **2024**, *12*, 1349864. [[CrossRef](#)]
26. Kötz, R.; Hahn, M.; Gallay, R. Temperature behavior and impedance fundamentals of supercapacitors. *J. Power Sources* **2006**, *154*, 550–555. [[CrossRef](#)]
27. Likitchatchawankun, A.; Whang, G.; Lau, J.; Munteshari, O.; Dunn, B.; Pilon, L. Effect of temperature on irreversible and reversible heat generation rates in ionic liquid-based electric double layer capacitors. *Electrochim. Acta* **2020**, *338*, 135802. [[CrossRef](#)]
28. Thomas, M.; Veleva, S.; Karamanova, B.; Brigandì, A.; Rey-Raap, N.; Arenillas, A.; Stoyanova, A.; Lufrano, F. Highly stable and reliable asymmetric solid-state supercapacitors with low self-discharge rates. *Sustain. Mater. Technol.* **2023**, *38*, e00770. [[CrossRef](#)]
29. Nishida, T.; Tashiro, Y.; Yamamoto, M. Physical and electrochemical properties of 1-alkyl-3-methylimidazolium tetrafluoroborate for electrolyte. *J. Fluor. Chem.* **2003**, *120*, 135–141. [[CrossRef](#)]
30. Kazemiabnavi, S.; Zhang, Z.; Thornton, K.; Banerjee, S. Electrochemical Stability Window of Imidazolium-Based Ionic Liquids as Electrolytes for Lithium Batteries. *J. Phys. Chem. B* **2016**, *120*, 5691–5702. [[CrossRef](#)]
31. Yamada, Y.; Furukawa, K.; Sodeyama, K.; Kikuchi, K.; Yaegashi, M.; Tateyama, Y.; Yamada, A. Unusual Stability of Acetonitrile-Based Superconcentrated Electrolytes for Fast-Charging Lithium-Ion Batteries. *J. Am. Chem. Soc.* **2014**, *136*, 5039–5046. [[CrossRef](#)]
32. Kim, E.; Han, J.; Ryu, S.; Choi, Y.; Yoo, J. Ionic Liquid Electrolytes for Electrochemical Energy Storage Devices. *Materials* **2021**, *14*, 4000. [[CrossRef](#)]
33. Karuppasamy, K.; Theerthagiri, J.; Vikraman, D.; Yim, C.-J.; Hussain, S.; Sharma, R.; Maiyalagan, T.; Qin, J.; Kim, H.-S. Ionic Liquid-Based Electrolytes for Energy Storage Devices: A Brief Review on Their Limits and Applications. *Polymers* **2020**, *12*, 918. [[CrossRef](#)]
34. Salanne, M. Ionic Liquids for Supercapacitor Applications. *Top. Curr. Chem.* **2017**, *375*, 63. [[CrossRef](#)]
35. Xu, C.; Li, B.; Du, H.; Kang, F.; Zeng, Y. Supercapacitive studies on amorphous MnO<sub>2</sub> in mild solutions. *J. Power Sources* **2008**, *184*, 691–694. [[CrossRef](#)]
36. Sudhan, N.; Subramani, K.; Karnan, M.; Ilayaraja, N.; Sathish, M. Biomass-Derived Activated Porous Carbon from Rice Straw for a High-Energy Symmetric Supercapacitor in Aqueous and Non-aqueous Electrolytes. *Energy Fuels* **2017**, *31*, 977–985. [[CrossRef](#)]
37. Karnan, M.; Subramani, K.; Sudhan, N.; Ilayaraja, N.; Sathish, M. Aloe vera Derived Activated High-Surface-Area Carbon for Flexible and High-Energy Supercapacitors. *ACS Appl. Mater. Interfaces* **2016**, *8*, 35191–35202. [[CrossRef](#)]
38. Subramani, K.; Sudhan, N.; Karnan, M.; Sathish, M. Orange Peel Derived Activated Carbon for Fabrication of High-Energy and High-Rate Supercapacitors. *ChemistrySelect* **2017**, *2*, 11384–11392. [[CrossRef](#)]
39. Boujibar, O.; Ghamous, F.; Ghosh, A.; Achak, O.; Chafik, T. Activated carbon with exceptionally high surface area and tailored nanoporosity obtained from natural anthracite and its use in supercapacitors. *J. Power Sources* **2019**, *436*, 226882. [[CrossRef](#)]
40. Wang, Y.; Hao, L.; Zeng, Y.; Cao, X.; Huang, H.; Liu, J.; Chen, X.; Wei, S.; Gan, L.; Yang, P.; et al. Three-dimensional hierarchical porous carbon derived from resorcinol formaldehyde-zinc tartrate/poly(styrene-maleic anhydride) for high performance supercapacitor electrode. *J. Alloys Compd.* **2021**, *886*, 161176. [[CrossRef](#)]
41. Wang, Y.; Zeng, Y.; Zhu, J.; Yang, C.; Huang, H.; Chen, X.; Wang, R.; Yan, P.; Wei, S.; Liu, M.; et al. From dual-aerogels with semi-interpenetrating polymer network structure to hierarchical porous carbons for advanced supercapacitor electrodes. *Colloids Surf. A Physicochem. Eng. Asp.* **2022**, *649*, 12935. [[CrossRef](#)]
42. Zaccagnini, P.; Serrapede, M.; Armandi, M.; Bianco, S.; Carminati, S.; Zampato, M.; Melis, G.; Pirri, C.F.; Lamberti, A. A high-temperature high-pressure supercapacitor based on ionic liquids for harsh environment applications. *Electrochim. Acta* **2023**, *447*, 142124. [[CrossRef](#)]
43. Penner, R.; Martin, C. Electrochemical investigations of electronically conductive polymers. 2. Evaluation of charge-transport rates in polypyrrole using an alternating current impedance method. *Phys. Chem.* **1989**, *93*, 984–989. [[CrossRef](#)]
44. Ahuja, P.; Sahu, V.; Ujjain, S.K.; Sharma, R.K.; Singh, G. Performance evaluation of Asymmetric Supercapacitor based on Cobalt manganite modified graphene nanoribbons. *Electrochim. Acta* **2014**, *14*, 429–436. [[CrossRef](#)]
45. Ahuja, P.; Ujjain, S.K.; Kanodia, R. Electrochemical behaviour of manganese & ruthenium mixed oxide@ reduced graphene oxide nanoribbon composite in symmetric and asymmetric supercapacitor. *Appl. Surf. Sci.* **2018**, *427 Pt A*, 102–111. [[CrossRef](#)]
46. KVan Aken, K.L.; McDonough, J.K.; Li, S.; Feng, G.; Chathoth, S.M.; Mamontov, E.; Fulvio, P.F.; Cummings, P.T.; Dai, S.; Gogotsi, Y. Effect of cation on diffusion coefficient of ionic liquids at onion-like carbon electrodes. *J. Phys. Condens. Matter* **2014**, *26*, 284104. [[CrossRef](#)]

**Disclaimer/Publisher's Note:** The statements, opinions and data contained in all publications are solely those of the individual author(s) and contributor(s) and not of MDPI and/or the editor(s). MDPI and/or the editor(s) disclaim responsibility for any injury to people or property resulting from any ideas, methods, instructions or products referred to in the content.